PHYSICAL REVIEW D **96,** 013003 (2017)

Theoretical description of the decays $\Lambda_b \to \Lambda^{(*)}(\frac{1}{2}^{\pm},\frac{3}{2}^{\pm}) + J/\psi$

Thomas Gutsche,[1] Mikhail A. Ivanov,[2] Jürgen G. Körner,[3] Valery E. Lyubovitskij,[1,4,5,6] Vladimir V. Lyubushkin,[7] and Pietro Santorelli[8,9]

[1]*Institut für Theoretische Physik, Universität Tübingen, Kepler Center for Astro and Particle Physics, Auf der Morgenstelle 14, D-72076 Tübingen, Germany*

[2]*Bogoliubov Laboratory of Theoretical Physics, Joint Institute for Nuclear Research, 141980 Dubna, Russia*

[3]*PRISMA Cluster of Excellence, Institut für Physik, Johannes Gutenberg-Universität, D-55099 Mainz, Germany*

[4]*Departamento de Física y Centro Científico Tecnológico de Valparaíso (CCTVal), Universidad Técnica Federico Santa María, Casilla 110-V Valparaíso, Chile*

[5]*Department of Physics, Tomsk State University, 634050 Tomsk, Russia*

[6]*Laboratory of Particle Physics, Mathematical Physics Department, Tomsk Polytechnic University, 634050 Tomsk, Russia*

[7]*Dzhelepov Laboratory of Nuclear Problems, Joint Institute for Nuclear Research, 141980 Dubna, Russia*

[8]*Dipartimento di Fisica, Università di Napoli Federico II, Complesso Universitario di Monte S. Angelo, Via Cintia, Edificio 6, 80126 Napoli, Italy*

[9]*Istituto Nazionale di Fisica Nucleare, Sezione di Napoli, 80126 Napoli, Italy*

(Received 20 May 2017; published 13 July 2017)

We calculate the invariant and helicity amplitudes for the transitions $\Lambda_b \to \Lambda^{(*)}(J^P) + J/\psi$, where the $\Lambda^{(*)}(J^P)$ are $\Lambda(sud)$-type ground and excited states with J^P quantum numbers $J^P = \frac{1}{2}^{\pm}, \frac{3}{2}^{\pm}$. The calculations are performed in the framework of a covariant confined quark model previously developed by us. We find that the values of the helicity amplitudes for the $\Lambda^*(1520,\frac{3}{2}^-)$ and the $\Lambda^*(1890,\frac{3}{2}^+)$ are suppressed compared with those for the ground state $\Lambda(1116,\frac{1}{2}^+)$ and the excited state $\Lambda^*(1405,\frac{1}{2}^-)$. This analysis is important for the identification of the hidden charm pentaquark states $P_c^+(4380)$ and $P_c^+(4450)$ which were discovered in the decay chain $\Lambda_b^0 \to P_c^+(\to pJ/\psi) + K^-$ because the cascade decay chain $\Lambda_b \to \Lambda^*(\frac{3}{2}^{\pm})(\to pK^-) + J/\psi$ involves the same final state.

DOI: 10.1103/PhysRevD.96.013003

I. INTRODUCTION

Recently the LHCb Collaboration has performed an angular analysis of the decay $\Lambda_b \to \Lambda^{(*)} + J/\psi$, where the Λ_b's are produced in pp collisions at $\sqrt{s} = 7$ TeV at the LHC (CERN) [1]. They reported on the measurement of the relative magnitude of the helicity amplitudes in the decay $\Lambda_b \to \Lambda^{(*)} + J/\psi$ by a fit to several asymmetry parameters in the cascade decay distribution $\Lambda_b \to \Lambda(\to p\pi^-) + J/\psi(\to \ell^+\ell^-)$ and $\Lambda_b \to \Lambda^*(\to pK^-) + J/\psi(\to \ell^+\ell^-)$.

In an earlier paper [2], we have performed a detailed analysis of the decay process $\Lambda_b \to \Lambda + J/\psi$ within a covariant quark model. We have worked out two variants of the threefold joint angular decay distributions in the cascade decay $\Lambda_b \to \Lambda(\to p\pi^-) + J/\psi(\to \ell^+\ell^-)$ for polarized and unpolarized Λ_b decays. We have further listed results on helicity amplitudes which determine the rate and the asymmetry parameters in the decay processes $\Lambda_b \to \Lambda(\to p\pi^-) + J/\psi$ and $\Lambda_b \to \Lambda(\to p\pi^-) + \psi(2S)$.

In this paper, we calculate the corresponding invariant and helicity amplitudes in the transitions $\Lambda_b \to \Lambda^{(*)}(J^P) + J/\psi$ where the $\Lambda^{(*)}(J^P)$ are Λ-type (sud) ground and excited states with J^P quantum numbers $J^P = \frac{1}{2}^{\pm}, \frac{3}{2}^{\pm}$. The calculations are performed in the framework of our covariant confined quark model developed previously by us. We find that the values of the helicity amplitudes for the $\Lambda_b \to \Lambda^*(1520,\frac{3}{2}^-)$, $\Lambda^*(1890,\frac{3}{2}^+)$ transitions are suppressed compared with those for the transitions to the ground state $\Lambda(1116,\frac{1}{2}^+)$ also calculated in [2] and the excited state $\Lambda^*(1405,\frac{1}{2}^-)$. This analysis is important for the identification of the hidden charm pentaquark states $P_c^+(4380)$ and $P_c^+(4450)$ since the cascade decay $\Lambda_b \to \Lambda^*(\frac{1}{2}^-,\frac{3}{2}^{\pm})(\to pK^-) + J/\psi$ involves the same final states as the decay $\Lambda_b^0 \to P_c^+(\to pJ/\psi) + K^-$. The subject of the hidden charm pentaquark states has been intensively discussed in the literature (see e.g. [3–10]).

Our paper is structured as follows. In Sec. II, we give explicit expressions for the hadronic matrix elements $\langle \Lambda_2|\bar{s}O^\mu b|\Lambda_1\rangle$ in terms of dimensionless invariant form factors $F_i^{V/A}(q^2)$. The corresponding vector and axial helicity amplitudes are linearly related to the invariant form factors. The linear relations are explicitly calculated and listed. The helicity amplitudes are the basic building blocks in the calculation of the rate and in the construction of the full angular decay distributions for the cascade decays.

In Sec. III, we construct local interpolating three-quark currents corresponding to the $\Lambda^{(*)}$ states with parity $J^P = \frac{1}{2}^{\pm}, \frac{3}{2}^{\pm}$. We then use nonlocal variants of the local interpolating currents to evaluate all invariant amplitudes in the framework of the covariant confined quark model. In Sec. IV, we give numerical results for the normalized helicity amplitudes and branching ratios. Finally, in Sec. V, we summarize our findings.

II. THE DECAYS $\Lambda_b \to \Lambda^{(*)}(\frac{1}{2}^{\pm}, \frac{3}{2}^{\pm}) + J/\psi$: MATRIX ELEMENT AND HELICITY AMPLITUDES

The matrix element of the exclusive decay $\Lambda_1(p_1,\lambda_1) \to \Lambda_2(p_2,\lambda_2) + V(q,\lambda_V)$ is defined by (in the present application the vector meson label V stands for the J/Ψ)

$$M(\Lambda_1 \to \Lambda_2 + V) = \frac{G_F}{\sqrt{2}} V_{cb} V_{cs}^* C_{\rm eff} f_V M_V \langle \Lambda_2 | \bar{s} O_\mu b | \Lambda_1 \rangle \epsilon^{\dagger\mu}(\lambda_V), \quad (1)$$

where M_V and f_V are the mass and the leptonic decay constant of the vector meson V, $O^\mu = \gamma^\mu(1-\gamma^5)$ and $|V_{cb}| = 0.0406$ and $|V_{cs}^*| = 0.974642$ are Cabibbo-Kabayashi-Maskawa (CKM) matrix elements. The coefficient $C_{\rm eff}$ stands for the combination of Wilson coefficients

$$C_{\rm eff} = C_1 + C_3 + C_5 + \xi(C_2 + C_4 + C_6). \quad (2)$$

The color factor $\xi = 1/N_c$ will be set to zero such that we only keep the leading term in the $1/N_c$–expansion. We take the numerical values of the Wilson coefficients from [11]:

$$C_1 = -0.257, \quad C_2 = 1.009, \quad C_3 = -0.005,$$
$$C_4 = -0.078, \quad C_5 \simeq 0, \quad C_6 = 0.001. \quad (3)$$

The hadronic matrix element $\langle \Lambda_2 | \bar{s} O^\mu b | \Lambda_1 \rangle$ is expressed in terms of six and eight, respectively, dimensionless invariant form factors $F_i^{V/A}(q^2)$ viz.

Transition $\frac{1}{2}^+ \to \frac{1}{2}^+$:

$$\langle \Lambda_2 | \bar{s}\gamma_\mu b | \Lambda_1 \rangle = \bar{u}(p_2,s_2)\left[\gamma_\mu F_1^V(q^2) - i\sigma_{\mu\nu}\frac{q_\nu}{M_1}F_2^V(q^2) + \frac{q_\mu}{M_1}F_3^V(q^2)\right]u(p_1,s_1)$$
$$\langle \Lambda_2 | \bar{s}\gamma_\mu\gamma_5 b | \Lambda_1 \rangle = \bar{u}(p_2,s_2)\left[\gamma_\mu F_1^A(q^2) - i\sigma_{\mu\nu}\frac{q_\nu}{M_1}F_2^A(q^2) + \frac{q_\mu}{M_1}F_3^A(q^2)\right]\gamma_5 u(p_1,s_1)$$

Transition $\frac{1}{2}^+ \to \frac{1}{2}^-$:

$$\langle \Lambda_2 | \bar{s}\gamma_\mu b | \Lambda_1 \rangle = \bar{u}(p_2,s_2)\left[\gamma_\mu F_1^V(q^2) - i\sigma_{\mu\nu}\frac{q_\nu}{M_1}F_2^V(q^2) + \frac{q_\mu}{M_1}F_3^V(q^2)\right]\gamma_5 u(p_1,s_1)$$
$$\langle \Lambda_2 | \bar{s}\gamma_\mu\gamma_5 b | \Lambda_1 \rangle = \bar{u}(p_2,s_2)\left[\gamma_\mu F_1^A(q^2) - i\sigma_{\mu\nu}\frac{q_\nu}{M_1}F_2^A(q^2) + \frac{q_\mu}{M_1}F_3^A(q^2)\right]u(p_1,s_1)$$

Transition $\frac{1}{2}^+ \to \frac{3}{2}^+$:

$$\langle \Lambda_2^* | \bar{s}\gamma_\mu b | \Lambda_1 \rangle = \bar{u}^\alpha(p_2,s_2)\left[g_{\alpha\mu}F_1^V(q^2) + \gamma_\mu\frac{p_{1\alpha}}{M_1}F_2^V(q^2) + \frac{p_{1\alpha}p_{2\mu}}{M_1^2}F_3^V(q^2) + \frac{p_{1\alpha}q_\mu}{M_1^2}F_4^V(q^2)\right]\gamma_5 u(p_1,s_1)$$
$$\langle \Lambda_2^* | \bar{s}\gamma_\mu\gamma_5 b | \Lambda_1 \rangle = \bar{u}^\alpha(p_2,s_2)\left[g_{\alpha\mu}F_1^A(q^2) + \gamma_\mu\frac{p_{1\alpha}}{M_1}F_2^A(q^2) + \frac{p_{1\alpha}p_{2\mu}}{M_1^2}F_3^A(q^2) + \frac{p_{1\alpha}q_\mu}{M_1^2}F_4^A(q^2)\right]u(p_1,s_1)$$

Transition $\frac{1}{2}^+ \to \frac{3}{2}^-$:

$$\langle \Lambda_2^* | \bar{s}\gamma_\mu b | \Lambda_1 \rangle = \bar{u}^\alpha(p_2,s_2)\left[g_{\alpha\mu}F_1^V(q^2) + \gamma_\mu\frac{p_{1\alpha}}{M_1}F_2^V(q^2) + \frac{p_{1\alpha}p_{2\mu}}{M_1^2}F_3^V(q^2) + \frac{p_{1\alpha}q_\mu}{M_1^2}F_4^V(q^2)\right]u(p_1,s_1)$$
$$\langle \Lambda_2^* | \bar{s}\gamma_\mu\gamma_5 b | \Lambda_1 \rangle = \bar{u}^\alpha(p_2,s_2)\left[g_{\alpha\mu}F_1^A(q^2) + \gamma_\mu\frac{p_{1\alpha}}{M_1}F_2^A(q^2) + \frac{p_{1\alpha}p_{2\mu}}{M_1^2}F_3^A(q^2) + \frac{p_{1\alpha}q_\mu}{M_1^2}F_4^A(q^2)\right]\gamma_5 u(p_1,s_1)$$

where $\sigma_{\mu\nu} = (i/2)(\gamma_\mu\gamma_\nu - \gamma_\nu\gamma_\mu)$ and all γ matrices are defined as in the text book by Bjorken-Drell. We use the same notation for the form factors $F_i^{V/A}$ in all transitions even though their numerical values differ. For completeness we have kept the form factors $F_3^{V/A}$ in the $\frac{1}{2}^+ \to \frac{1}{2}^\pm$ transitions and $F_4^{V/A}$ in the $\frac{1}{2}^+ \to \frac{3}{2}^\pm$ transitions although they do not contribute to the decay $\Lambda_b \to \Lambda^{(*)} + J/\psi$ since $q_\mu \epsilon_V^\mu = 0$.

Next we express the vector and axial helicity amplitudes $H_{\lambda_2\lambda_V}$ in terms of the invariant form factors $F_i^{V/A}$, where $\lambda_V = \pm 1, 0$ and $\lambda_2 = \pm 1/2, \pm 3/2$ are the helicity components of the vector meson V and the daughter baryon Λ_2, respectively. Note again that the time-component helicity amplitudes $H^{V,A}_{\lambda_2 t}$ do not contribute since the J/ψ is a spin 1 meson. We need to calculate the expressions

$$H_{\lambda_2\lambda_V} = \langle \Lambda_2(p_2,\lambda_2)|\bar{s}O_\mu b|\Lambda_1(p_1,\lambda_1)\rangle \epsilon^{\dagger\mu}(\lambda_V) = H^V_{\lambda_2\lambda_V} - H^A_{\lambda_2\lambda_V}, \quad (4)$$

where we split the helicity amplitudes into their vector and axial parts. We shall work in the rest frame of the parent baryon Λ_1 with the daughter baryon Λ_2 moving in the positive z-direction: $p_1 = (M_1, \vec{\mathbf{0}})$, $p_2 = (E_2, 0, 0, |\mathbf{p}_2|)$ and $q = (q_0, 0, 0, -|\mathbf{p}_2|)$. In this case, $\lambda_1 = \lambda_2 - \lambda_V$. Following Ref. [12] one has

Transition $\frac{1}{2}^+ \to \frac{1}{2}^+$: $H^V_{-\lambda_2,-\lambda_V} = +H^V_{\lambda_2,\lambda_V}$ and $H^A_{-\lambda_2,-\lambda_V} = -H^A_{\lambda_2,\lambda_V}$.

$$H^V_{\frac{1}{2}t} = \sqrt{Q_+/q^2}\left(F_1^V M_- + F_3^V \frac{q^2}{M_1}\right) \qquad H^A_{\frac{1}{2}t} = \sqrt{Q_-/q^2}\left(F_1^A M_+ - F_3^A \frac{q^2}{M_1}\right)$$
$$H^V_{\frac{1}{2}0} = \sqrt{Q_-/q^2}\left(F_1^V M_+ + F_2^V \frac{q^2}{M_1}\right) \qquad H^A_{\frac{1}{2}0} = \sqrt{Q_+/q^2}\left(F_1^A M_- - F_2^A \frac{q^2}{M_1}\right)$$
$$H^V_{\frac{1}{2}1} = \sqrt{2Q_-}\left(-F_1^V - F_2^V \frac{M_+}{M_1}\right) \qquad H^A_{\frac{1}{2}1} = \sqrt{2Q_+}\left(-F_1^A + F_2^A \frac{M_-}{M_1}\right)$$

Transition $\frac{1}{2}^+ \to \frac{1}{2}^-$: $H^V_{-\lambda_2,-\lambda_V} = -H^V_{\lambda_2,\lambda_V}$ and $H^A_{-\lambda_2,-\lambda_V} = +H^A_{\lambda_2,\lambda_V}$.

$$H^V_{\frac{1}{2}t} = \sqrt{Q_-/q^2}\left(F_1^V M_+ - F_3^V \frac{q^2}{M_1}\right) \qquad H^A_{\frac{1}{2}t} = \sqrt{Q_+/q^2}\left(F_1^A M_- + F_3^A \frac{q^2}{M_1}\right)$$
$$H^V_{\frac{1}{2}0} = \sqrt{Q_+/q^2}\left(F_1^V M_- - F_2^V \frac{q^2}{M_1}\right) \qquad H^A_{\frac{1}{2}0} = \sqrt{Q_-/q^2}\left(F_1^A M_+ + F_2^A \frac{q^2}{M_1}\right)$$
$$H^V_{\frac{1}{2}1} = \sqrt{2Q_+}\left(-F_1^V + F_2^V \frac{M_-}{M_1}\right) \qquad H^A_{\frac{1}{2}1} = \sqrt{2Q_-}\left(-F_1^A - F_2^A \frac{M_+}{M_1}\right)$$

Transition $\frac{1}{2}^+ \to \frac{3}{2}^+$: $H^V_{-\lambda_2,-\lambda_V} = -H^V_{\lambda_2,\lambda_V}$ and $H^A_{-\lambda_2,-\lambda_V} = +H^A_{\lambda_2,\lambda_V}$.

$$H^V_{\frac{1}{2}t} = -\sqrt{\frac{2}{3}\cdot\frac{Q_+}{q^2}}\frac{Q_-}{2M_1M_2}\left(F_1^V M_1 - F_2^V M_+ + F_3^V \frac{M_+M_- - q^2}{2M_1} + F_4^V \frac{q^2}{M_1}\right)$$
$$H^V_{\frac{1}{2}0} = -\sqrt{\frac{2}{3}\cdot\frac{Q_-}{q^2}}\left(F_1^V \frac{M_+M_- - q^2}{2M_2} - F_2^V \frac{Q_+M_-}{2M_1M_2} + F_3^V \frac{|\mathbf{p_2}|^2}{M_2}\right)$$
$$H^V_{\frac{1}{2}1} = \sqrt{\frac{Q_-}{3}}\left(F_1^V - F_2^V \frac{Q_+}{M_1M_2}\right) \qquad H^V_{\frac{3}{2}1} = -\sqrt{Q_-}F_1^V$$
$$H^A_{\frac{1}{2}t} = \sqrt{\frac{2}{3}\cdot\frac{Q_-}{q^2}}\frac{Q_+}{2M_1M_2}\left(F_1^A M_1 + F_2^A M_- + F_3^A \frac{M_+M_- - q^2}{2M_1} + F_4^A \frac{q^2}{M_1}\right)$$
$$H^A_{\frac{1}{2}0} = \sqrt{\frac{2}{3}\cdot\frac{Q_+}{q^2}}\left(F_1^A \frac{M_+M_- - q^2}{2M_2} + F_2^A \frac{Q_-M_+}{2M_1M_2} + F_3^A \frac{|\mathbf{p_2}|^2}{M_2}\right)$$
$$H^A_{\frac{1}{2}1} = \sqrt{\frac{Q_+}{3}}\left(F_1^A - F_2^A \frac{Q_-}{M_1M_2}\right) \qquad H^A_{\frac{3}{2}1} = \sqrt{Q_+}F_1^A$$

Transition $\frac{1}{2}^+ \to \frac{3}{2}^-$: $H^V_{-\lambda_2,-\lambda_V} = +H^V_{\lambda_2,\lambda_V}$ and $H^A_{-\lambda_2,-\lambda_V} = -H^A_{\lambda_2,\lambda_V}$.

$$H^V_{\frac{1}{2}t} = \sqrt{\frac{2}{3}\cdot\frac{Q_-}{q^2}}\frac{Q_+}{2M_1M_2}\left(F_1^V M_1 + F_2^V M_- + F_3^V\frac{M_+M_- - q^2}{2M_1} + F_4^V\frac{q^2}{M_1}\right)$$

$$H^V_{\frac{1}{2}0} = \sqrt{\frac{2}{3}\cdot\frac{Q_+}{q^2}}\left(F_1^V\frac{M_+M_- - q^2}{2M_2} + F_2^V\frac{Q_-M_+}{2M_1M_2} + F_3^V\frac{|\mathbf{p_2}|^2}{M_2}\right)$$

$$H^V_{\frac{1}{2}1} = \sqrt{\frac{Q_+}{3}}\left(F_1^V - F_2^V\frac{Q_-}{M_1M_2}\right) \qquad H^V_{\frac{3}{2}1} = \sqrt{Q_+}F_1^V$$

$$H^A_{\frac{1}{2}t} = -\sqrt{\frac{2}{3}\cdot\frac{Q_+}{q^2}}\frac{Q_-}{2M_1M_2}\left(F_1^A M_1 - F_2^A M_+ + F_3^A\frac{M_+M_- - q^2}{2M_1} + F_4^A\frac{q^2}{M_1}\right)$$

$$H^A_{\frac{1}{2}0} = -\sqrt{\frac{2}{3}\cdot\frac{Q_-}{q^2}}\left(F_1^A\frac{M_+ - M_- - q^2}{2M_2} - F_2^A\frac{Q_+M_-}{2M_1M_2} + F_3^A\frac{|\mathbf{p_2}|^2}{M_2}\right)$$

$$H^A_{\frac{1}{2}1} = \sqrt{\frac{Q_-}{q^2}}\left(F_1^A - F_2^A\frac{Q_+}{M_1M_2}\right) \qquad H^A_{\frac{3}{2}1} = -\sqrt{Q_-}F_1^A$$

We use the abbreviations $M_\pm = M_1 \pm M_2$, $Q_\pm = M_\pm^2 - q^2$, $|\mathbf{p_2}| = \lambda^{1/2}(M_1^2, M_2^2, q^2)/(2M_1)$.

For the decay width one finds

$$\Gamma(\Lambda_b \to \Lambda^* + V) = \frac{G_F^2}{32\pi}\frac{|\mathbf{p_2}|}{M_1^2}|V_{cb}V_{cs}^*|^2 C_{\rm eff}^2 f_V^2 M_V^2 \mathcal{H}_N \quad (5)$$

$$\mathcal{H}_N = \sum_{\lambda_2,\lambda_V}|H_{\lambda_2,\lambda_V}|^2 \quad (6)$$

The sum over helicities includes all helicities satisfying the angular momentum constraint $|\lambda_2 - \lambda_v| \le 1/2$. Compared to Eq. (11) of [2], we have dropped a factor containing the lepton mass in the rate expression.

Using the helicity amplitudes one can write down angular decay distributions in the cascade decays $\Lambda_b \to \Lambda^{(*)}(\to B + M) + J/\psi(\to \ell^+\ell^-)$ where B and M are the final baryon (N, Σ, etc.) and meson (π, K, etc.) states. Note that the decays $\Lambda^* \to pK^-$ are strong and therefore parity conserving while the decay $\Lambda \to p\pi^-$ is a weak decay and therefore parity violating. The angular decay distribution involving the strong decays $\Lambda^* \to pK^-$ can be obtained from that involving the weak decay $\Lambda \to p\pi^-$ by setting the relevant asymmetry parameter to zero. When the Λ_b is polarized the angular decay distributions are characterized by three polar angles and two azimuthal angles. The full five-fold angular decay distribution can be found in [13–15]. Corresponding three-fold polar angle distributions for polarized Λ_b decay and a three-fold joint decay distribution for unpolarized Λ_b decay can be obtained from the full five-fold decay distributions written down in [14,15] by appropriate angular integrations or by setting the polarization of the Λ_b to zero.

As mentioned in the introduction there are two variants of how the angular decay distributions of such cascade decay processes can be presented. The unprocessed form the angular decay distribution $W(\Omega_1, \Omega_2, \theta)$ is written down directly from the traces of the production and the rotated decay spin density matrices. In the present case, Ω_1 describes the relative orientation of the decay $\Lambda \to p\pi^-$ (or $\Lambda^* \to pK^-$), Ω_2 the relative orientation of the leptonic decay $J/\psi \to \ell^+\ell^-$ and θ the polar orientation of the polarization of the Λ_b. In the normal form, one subtracts off unity corresponding to the normalized total rate; i.e., one writes

$$W(\Omega_1, \Omega_2, \theta) = 1 + \tilde{W}(\Omega_1, \Omega_2, \theta) \quad (7)$$

where $\int d\Omega_1 d\Omega_2 d\cos\theta \tilde{W}(\Omega_1, \Omega_2, \theta) = 0$. The normal form of the threefold angular decay distribution $\tilde{W}(\theta_1, \theta_2, \theta)$ can be written in terms of three linear combinations of normalized squared helicity amplitudes $|\hat{H}_{\lambda_2\lambda_V}|^2$ which are [1,2]

$$\alpha_b = |\hat{H}_{+\frac{1}{2}0}|^2 - |\hat{H}_{-\frac{1}{2}0}|^2 + |\hat{H}_{-\frac{1}{2}-1}|^2 - |\hat{H}_{+\frac{1}{2}+1}|^2 - (|\hat{H}_{-\frac{3}{2}-1}|^2 - |\hat{H}_{+\frac{3}{2}+1}|^2), \quad (8)$$

$$r_0 = |\hat{H}_{+\frac{1}{2}0}|^2 + |\hat{H}_{-\frac{1}{2}0}|^2, \qquad r_1 = |\hat{H}_{+\frac{1}{2}0}|^2 - |\hat{H}_{-\frac{1}{2}0}|^2, \quad (9)$$

where $|\hat{H}_{\lambda_2\lambda_V}|^2 = |H_{\lambda_2\lambda_V}|^2/\mathcal{H}_N$. The last bracketed contribution in (8) only comes in for the $1/2^+ \to 3/2^\pm$ case.

III. THE $\Lambda_b \to \Lambda^{(*)}$ FORM FACTORS IN THE COVARIANT QUARK MODEL

We employ generic three-quark currents to describe the $\Lambda_Q(J^P)$ states:

TABLE I. Currents for the $[ud]$ diquark states.

State	Current	J^P
Scalar diquark	$u^T_{a_2} C\gamma_5 d_{a_3}$	0^+
Pseudoscalar diquark	$u^T_{a_2} C d_{a_3}$	0^-
Vector diquark	$u^T_{a_2} C\gamma_5\gamma_\mu d_{a_3}$	1^-
Axial-vector diquark	$u^T_{a_2} C\gamma_\mu d_{a_3}$	1^+

$$\Lambda_Q(J^P) \Rightarrow \epsilon_{a_1a_2a_3}\Gamma_1 Q_{a_1}(u_{a_2} C\Gamma_2 d_{a_3}). \tag{10}$$

Here $Q = b$ or s, the color index is denoted by a_i and $C = \gamma^0\gamma^2$ is the charge conjugation matrix. The Dirac matrices Γ_1 and Γ_2 are chosen in such a way to provide the correct P-parity for the Λ-baryons. A set of currents for the flavor-antisymmetric $[ud]$ diquark states is shown in Table I by analogy with the classification given in Ref. [16].

One can then construct local three-quark currents with the appropriate quantum numbers of the $\Lambda_Q(\frac{1}{2}^\pm, \frac{3}{2}^\pm)$ states. They are given by

$$\begin{aligned}
\Lambda_Q^{1/2^+} &\Rightarrow \epsilon_{a_1a_2a_3} Q_{a_1}(u_{a_2} C\gamma_5 d_{a_3}),\\
\Lambda_Q^{1/2^-} &\Rightarrow \epsilon_{a_1a_2a_3}\gamma_5 Q_{a_1}(u_{a_2} C\gamma_5 d_{a_3}),\\
\Lambda_Q^{3/2^+} &\Rightarrow \epsilon_{a_1a_2a_3}\gamma_5 Q_{a_1}(u_{a_2} C\gamma_5\gamma_\mu d_{a_3}),\\
\Lambda_Q^{3/2^-} &\Rightarrow \epsilon_{a_1a_2a_3} Q_{a_1}(u_{a_2} C\gamma_5\gamma_\mu d_{a_3}).
\end{aligned} \tag{11}$$

Note that we do not employ derivative couplings in our interpolating currents. It would be interesting to find out whether the use of derivative couplings would change our results.

The covariant quark model employs nonlocal renditions of the local three-quark currents in Eq. (11). The nonlocal Lagrangian describing the couplings of the baryons Λ_Q ($Q = b$, s) with their constituent quarks is then given by

$$\begin{aligned}
\mathcal{L}^{\Lambda_Q}_{\rm int}(x) &= g_{\Lambda_Q}\bar{\Lambda}_Q(x)\cdot J_{\Lambda_Q}(x) + \text{H.c.},\\
J_{\Lambda_Q}(x) &= \int dx_1 \int dx_2 \int dx_3 F_{\Lambda_Q}(x; x_1, x_2, x_3)\epsilon_{a_1a_2a_3}\Gamma_1 Q_{a_1}(x_1)(u_{a_2}(x_2) C\Gamma_2 d_{a_3}(x_3)),\\
F_{\Lambda_Q}(x; x_1, x_2, x_3) &= \delta^{(4)}\left(x - \sum_{i=1}^{3} w_i x_i\right)\Phi_{\Lambda_Q}\left(\sum_{i<j}(x_i - x_j)^2\right),
\end{aligned} \tag{12}$$

where $w_i = m_i/(\sum_{j=1}^3 m_j)$ and m_i is the mass of the quark placed at the space-time point x_i.

First of all, one has to calculate the Λ_Q mass functions (or self-energy functions) arising from the interactions of the $\Lambda^{(*)}$ baryons with the constituent quarks as written down in Eq. (12). Then one can determine the coupling constants g_{Λ_Q} by using the so-called compositeness condition.

The Fourier-transforms of the mass functions are given by

$$\begin{aligned}
\bar{u}(p', s)\tilde{\Sigma}_{1/2^\pm}(p', p)u(p, s) &= +ig^2_{1/2^\pm}\int dx e^{ip'x}\int dy e^{-ipy}\bar{u}(p', s)\langle 0|T\{J_{1/2^\pm}(x)\bar{J}_{1/2^\pm}(y)\}|0\rangle u(p, s),\\
u_\mu(p', s)\tilde{\Sigma}^{\mu\nu}_{3/2^\pm}(p', p)u_\nu(p, s) &= -ig^2_{3/2^\pm}\int dx e^{ip'x}\int dy e^{-ipy}\bar{u}_\mu(p', s)\langle 0|T\{J^\mu_{3/2^\pm}(x)\bar{J}^\nu_{3/2^\pm}(y)\}|0\rangle u_\nu(p, s).
\end{aligned} \tag{13}$$

The calculation of the Fourier-transforms of the vertex functions Φ can be done in a straightforward way by using Jacobi coordinates. One arrives at the following expressions

$$\begin{aligned}
\tilde{\Sigma}(p', p) &= (2\pi)^4\delta^{(4)}(p' - p)\Sigma(p),\\
\Sigma(p) &= \pm 6g^2\int\frac{d^4k_1}{(2\pi)^4 i}\int\frac{d^4k_2}{(2\pi)^4 i}\tilde{\Phi}^2[-K^2]\Gamma_1 S_Q(k_1 + w_1 p)\Gamma_1\text{tr}[\Gamma_2 S_u(k_2 - w_2 p)\Gamma_2 S_d(k_2 - k_1 + w_3 p)],\\
K^2 &\equiv \frac{1}{2}(k_1 - k_2)^2 + \frac{1}{6}(k_1 + k_2)^2
\end{aligned} \tag{14}$$

where the "+" sign stands for the final baryon states with $J^P = \frac{1}{2}^+$ and $\frac{3}{2}^-$ and the "−" sign stands for the final baryon states with $J^P = \frac{1}{2}^-$ and $\frac{3}{2}^+$. We have omitted some unnecessary indices and self-explanatory notation.

In the numerical calculations, we choose a simple Gaussian form for the vertex functions (for both mesons and baryons):

$$\tilde{\Phi}(-P^2) = \exp(P^2/\Lambda^2) \equiv \exp(sP^2), \tag{15}$$

where Λ is a size parameter describing the distribution of the quarks inside a given hadron and $s \equiv 1/\Lambda^2$. We emphasize that the Minkowskian momentum variable P^2 turns into the Euclidean form $-P_E^2$ needed for the appropriate falloff behavior of the correlation function (15) in the Euclidean region.

The compositeness condition implies that the renormalization constant of the hadron wave function is set equal to zero. This condition has been suggested by Weinberg [17] and Salam [18] (for a review, see [19]) and extensively used in our approach (for details, see [20]). In the $J = 1/2$ case, the compositeness condition may be written in the form

$$Z_{1/2} = 1 - \Sigma'_{1/2}(\not{p}) = 0, \qquad \not{p} = M. \tag{16}$$

where $\Sigma'_{1/2}(\not{p})$ is the derivative of the mass function taken on the mass shell $p^2 = M^2$. In the $J = 3/2$ case, one has to account for the Rarita-Schwinger conditions $p^\alpha u_\alpha(p,s) = 0$ and $\gamma^\alpha u_\alpha(p,s) = 0$. This can be done by splitting off a scalar function in the form $\Sigma^{\mu\nu}_{3/2}(p) = g^{\mu\nu}\Sigma_{3/2}(\not{p})$. The compositeness condition for the $J = 3/2$ case reads

$$Z_{3/2} = 1 - \Sigma'_{3/2}(\not{p}) = 0, \qquad \not{p} = M. \tag{17}$$

In practice, it is more convenient to use a form equivalent to Eqs. (16) and (17) by writing

$$\frac{d\Sigma(\not{p})}{dp^\alpha} = \gamma^\alpha, \qquad p^\alpha = M\gamma^\alpha, \quad \text{and} \quad \not{p} = M. \tag{18}$$

The loop integrations in Eq. (14) are performed by using the Fock-Schwinger representations of the quark propagators. The tensorial loop integrations and the manipulations with Dirac matrices are performed with the help of FORM [21]. The final relations needed for the determination of the coupling constants may be symbolically cast in the form

$$\begin{aligned} g &= 1/\sqrt{G(M,s;m_q)}, \\ G(M,s;m_q) &= \int_0^{1/\lambda^2} dt t^2 \int d^3\alpha \delta\left(1 - \sum_{i=1}^{3}\alpha_i\right) \\ &\quad \times \tilde{G}(t\alpha_1, t\alpha_2, t\alpha_3; M, s, m_q) \\ &= \int_0^{1/\lambda^2} dt t^2 \int_0^1 d^2x x_1 \tilde{G}(t\alpha_1, t\alpha_2, t\alpha_3; M, s, m_q), \\ \alpha_1 &= 1 - x_1, \quad \alpha_2 = x_1(1-x_2), \quad \alpha_3 = x_1x_2. \end{aligned} \tag{19}$$

The infrared cutoff parameter λ provides for the absence of all constituent quark threshold singularities. The threefold integrals are calculated by a FORTRAN code using the NAG library.

The matrix elements of the transitions $\langle \Lambda_2|\bar{s}\Gamma_\mu b|\Lambda_1\rangle$ finally read

$$\begin{aligned} \langle \Lambda_2|\bar{s}\Gamma_\mu b|\Lambda_1\rangle &= 6g_{\Lambda_1}g_{\Lambda_2}\int \frac{d^4k_1}{(2\pi)^4 i}\int \frac{d^4k_2}{(2\pi)^4 i}\tilde{\Phi}_{\Lambda_1}[-\Omega_1^2]\tilde{\Phi}_{\Lambda_2}[-\Omega_2^2] \\ &\quad \times \bar{u}_2(p_2,s_2)\Gamma_1 S_s(k_1+p_2)\Gamma_\mu S_b(k_1+p_1)\mathrm{tr}[S_u(k_2)\Gamma_2 S_d(k_2-k_1)\gamma_5]u_1(p_1,s_1), \\ \Omega_1^2 &\equiv \frac{1}{2}(k_1 - k_2 + v_3p_1)^2 + \frac{1}{6}(k_1 + k_2 + (2v_2+v_3)p_1)^2, \\ \Omega_2^2 &\equiv \frac{1}{2}(k_1 - k_2 + w_3p_2)^2 + \frac{1}{6}(k_1 + k_2 + (2w_2+w_3)p_2)^2. \end{aligned} \tag{20}$$

where $\Gamma_\mu = \gamma_\mu$ or $\Gamma_\mu = \gamma_\mu\gamma_5$, $\Lambda_1 = \Lambda_b(p_1,s_1)$ and $\Lambda_2 = \Lambda^{(*)}(p_2,s_2)$. The reduced quark masses are defined by

$$\begin{aligned} &v_1 = \frac{m_b}{m_{bud}}, \qquad v_2 = \frac{m_u}{m_{bud}}, \qquad v_3 = \frac{m_d}{m_{bud}}, \\ &m_{bud} = m_b + m_u + m_d, \qquad w_1 = \frac{m_s}{m_{sdu}}, \qquad w_2 = \frac{m_u}{m_{sdu}}, \\ &w_3 = \frac{m_d}{m_{sdu}}, \qquad m_{sdu} = m_s + m_d + m_u. \end{aligned}$$

Below we show the different Dirac structures Γ_1 and Γ_2 in (20) for the different final state $\Lambda^{(*)}$ baryons:

J^P	$\Gamma_1 \otimes \Gamma_2$	J^P	$\Gamma_1 \otimes \Gamma_2$
$\frac{1}{2}^+$	$I \otimes \gamma_5$	$\frac{3}{2}^+$	$\gamma_5 \otimes \gamma_5\gamma_\alpha$
$\frac{1}{2}^-$	$\gamma_5 \otimes \gamma_5$	$\frac{3}{2}^-$	$I \otimes \gamma_5\gamma_\alpha$

The expressions for the scalar form factors are represented by the fourfold integrals

$$\begin{aligned} F(M_1,s_1,M_2,s_2,m_q,q^2) &= 6g_{\Lambda_1}g_{\Lambda_2}\int_0^{1/\lambda^2} dt t^3 \int_0^1 d^3x x_1^2 x_2 \tilde{F}(t\alpha_1,t\alpha_2,t\alpha_3,t\alpha_4;M_1,s_1,M_2,s_2,m_q,q^2), \\ \alpha_1 &= 1 - x_1, \qquad \alpha_2 = x_1(1-x_2), \qquad \alpha_3 = x_1x_2(1-x_3), \qquad \alpha_4 = x_1x_2x_3. \end{aligned}$$

The model parameters are the constituent quark masses m_q and the infrared cutoff parameter λ responsible for quark confinement. They are taken from a new fit done and used in our papers on the semileptonic $B \to D^{(*)}\ell\bar{\nu}_\ell$ decays [22–25], rare $B \to M\bar{\ell}\ell$ decays [26–28], the semileptonic decays $\Lambda_b \to \Lambda_c + \tau^- + \bar{\nu}_\tau$, $\Lambda_c^+ \to \Lambda\ell^+\nu_\ell$ [29,30] and for the calculation of nucleon tensor form factors [31]. The best fit values for the constituent quark masses and the infrared cutoff parameter λ are

$$\begin{array}{cccccc} m_u & m_s & m_c & m_b & \lambda & \\ \hline 0.241 & 0.428 & 1.67 & 5.05 & 0.181 & \text{GeV} \end{array}. \tag{21}$$

The dimensional-size parameters of the ground-state Λ_b and Λ_s baryons have been determined by a fit to the semileptonic decays $\Lambda_b \to \Lambda_c + \ell^-\bar{\nu}_\ell$ and $\Lambda_c \to \Lambda + \ell^+\nu_\ell$. The resulting values are $\Lambda_{\Lambda_b} = 0.571$, $\Lambda_{\Lambda_s} = 0.492$ GeV. The values of the size parameters of the final states $\Lambda^*(\frac{1}{2}^-, \frac{3}{2}^\pm)$ are set equal to the size parameter of the ground state Λ_{Λ_s}. For the size parameter of the J/ψ we take $\Lambda_{J/\psi} = 1.74$ GeV as determined from our most recent fit described above.

IV. NUMERICAL RESULTS

In Tables II and III, we list our predictions for the normalized helicity amplitudes and branching fractions.

The helicity amplitudes H_{λ_2,λ_V} of the produced $\Lambda^{(*)}$ states are clearly dominated by the helicity configuration $\lambda_2 = -1/2$ as in the quark level transition $b \to s$. For the spin $1/2$ states in the transition $1/2^+ \to 1/2^\pm$ this implies that the two $\Lambda^{(*)}(1/2)$ states are almost purely left-handed.

It is also apparent that the branching ratios involving the excited $J^P = 3/2^\pm$ states are suppressed relative to those of the ground state $\Lambda(1116)$ and the excited state with $J^P = 1/2^-$.

TABLE II. Moduli squared of normalized helicity amplitudes.

Λ^*	1116	1405	1890	1520
J^P	$\frac{1}{2}^+$	$\frac{1}{2}^-$	$\frac{3}{2}^+$	$\frac{3}{2}^-$
$\lvert\hat{H}_{+\frac{3}{2}+1}\rvert^2$	0	0	3.50×10^{-4}	0.84×10^{-4}
$\lvert\hat{H}_{+\frac{1}{2}+1}\rvert^2$	2.34×10^{-3}	1.27×10^{-2}	3.19×10^{-2}	2.26×10^{-2}
$\lvert\hat{H}_{+\frac{1}{2}0}\rvert^2$	3.24×10^{-4}	5.19×10^{-3}	1.61×10^{-3}	1.82×10^{-3}
$\lvert\hat{H}_{-\frac{1}{2}0}\rvert^2$	0.53	0.51	0.51	0.54
$\lvert\hat{H}_{-\frac{1}{2}-1}\rvert^2$	0.47	0.47	0.45	0.44
$\lvert\hat{H}_{-\frac{3}{2}-1}\rvert^2$	0	0	3.34×10^{-3}	1.06×10^{-3}

TABLE III. Branching ratio $\mathcal{B}(\Lambda_b \to \Lambda^* + J/\psi)$ (in units of 10^{-4}).

Λ^*	1116	1405	1890	1520
J^P	$\frac{1}{2}^+$	$\frac{1}{2}^-$	$\frac{3}{2}^+$	$\frac{3}{2}^-$
$\mathcal{B}\times10^4$	8.00	7.07	0.45	0.19

Next, we discuss the experimental results on the pentaquark evidence in light of our theoretical findings. Large data samples of the bottom baryon state Λ_b^0 were collected by the LHC experiments from pp collisions during Run I. An angular analysis of the decay $\Lambda_b^0 \to J/\psi(\mu^+\mu^-)\Lambda^0(p\pi^-)$ was first done by the LHCb Collaboration [1] and was then repeated by the ATLAS [32] and CMS [33] Collaborations. From Table IV, one can assess the present-day accuracy of the measured helicity amplitudes for the transition $\Lambda_b^0 \to \Lambda^0(J^P = 1/2^+)$.

The dominant production mechanism of the Λ_b^0's at the LHC proceeds via the strong interactions. Therefore the longitudinal polarization P_L of the produced Λ_b^0 vanishes because of parity conservation. Contrary to this a transverse polarization component P_T is not forbidden by parity. The P_T component depends strongly on the Feynman variable $x_F = 2p_\parallel/\sqrt{s}$, where $p_\parallel$ is the longitudinal momentum of the Λ_b^0 and $\sqrt{s}$ is the collision center-of-mass energy. For the collisions of identical unpolarized initial state particles one has $P_T(-x_F) = -P_T(x_F)$ by virtue of the invariance under the rotation of the coordinate system through an angle of 180° about the normal $\vec{n}$ to the reaction plane [34]. This implies that $P_T(x_F = 0) = 0$. Taking into account the very small value $x_F \approx 0.02$ for Λ_b^0's produced at the LHC at $\sqrt{s} = 7$ TeV, P_T is estimated to be $\mathcal{O}(10\%)$ in [35]. The P_T value measured in [1,32,33] is consistent with the expected value of zero. We therefore treat Λ_b^0 to be unpolarized in our further analysis.

Large samples of the decay $\Lambda_b^0 \to J/\psi K^- p$ decay have been collected by the LHCb experiment [36]. This decay was expected to be dominated by $\Lambda^\star$ resonances decaying into $K^- p$ final states. The measured fit fractions of the $\Lambda(1405)$ and $\Lambda(1520)$ states are $(15 \pm 1 \pm 6)\%$ and $(19 \pm 1 \pm 4)\%$, respectively. It was also found that the data cannot be satisfactorily described without the inclusion of two Breit-Wigner resonances decaying strongly to $J/\psi p$. These new pentaquark states, called $P_c(4380)^+$ and $P_c(4450)^+$, have large fit fractions of $(4.1 \pm 0.5 \pm 1.1)\%$ and $(8.4 \pm 0.7 \pm 4.2)\%$ of the total $\Lambda_b^0 \to J/\psi K^- p$ sample, respectively.

The presence of various conventional $\Lambda^\star \to K^- p$ resonances and exotic pentaquark states $P_c^+ \to J/\psi p$, which can interfere with each other, makes the analysis of experimental data particularly difficult and challenging. There are 32 complex parameters ($B_{L,S}$ amplitudes) which describe the transition $\Lambda_b^0 \to \Lambda^\star$. The 32 parameters were determined in a six-dimensional fit [36] to the angular decay distribution of the cascade decay process. Their numerical values for the default fit variant can be found in the Appendix G of [37].

The helicity amplitudes $H_{\lambda_2,\lambda_{J/\psi}}(\Lambda_b \to \Lambda^{(*)} J/\psi)$ used in the present approach are linearly related to the

TABLE IV. Asymmetry parameters and moduli squared of normalized helicity amplitudes $|\hat{H}_{\lambda_\Lambda\lambda_\psi}|^2$ for the $\Lambda_b^0 \to \Lambda^0$ transition.

$\Lambda^{(\star)}$, J^P	Λ, $\frac{1}{2}^+$			
Quantity	Our results	LHCb [1]	ATLAS [32]	CMS [33]
$\lvert\hat{H}_{+\frac{1}{2}+1}\rvert^2$	2.34×10^{-3}	$-0.10 \pm 0.04 \pm 0.03$	$(0.08^{+0.13}_{-0.08} \pm 0.06)^2$	$0.05 \pm 0.04 \pm 0.02$
$\lvert\hat{H}_{+\frac{1}{2}0}\rvert^2$	3.24×10^{-4}	$0.01 \pm 0.04 \pm 0.03$	$(0.17^{+0.12}_{-0.17} \pm 0.09)^2$	$-0.02 \pm 0.03 \pm 0.02$
$\lvert\hat{H}_{-\frac{1}{2}0}\rvert^2$	0.532	$0.57 \pm 0.06 \pm 0.03$	$(0.59^{+0.06}_{-0.07} \pm 0.03)^2$	$0.51 \pm 0.03 \pm 0.02$
$\lvert\hat{H}_{-\frac{1}{2}-1}\rvert^2$	0.465	$0.51 \pm 0.05 \pm 0.02$	$(0.79^{+0.04}_{-0.05} \pm 0.02)^2$	$0.46 \pm 0.02 \pm 0.02$
α_b	−0.069	$0.05 \pm 0.17 \pm 0.07$	$0.30 \pm 0.16 \pm 0.06$	$-0.12 \pm 0.13 \pm 0.06$
r_0	0.533	$0.58 \pm 0.02 \pm 0.01$		
r_1	−0.532	$-0.56 \pm 0.10 \pm 0.05$		

LS-amplitudes B_{LS} used in [36] (see e.g. [38,39]). The coefficients of this linear relation can be obtained with the help of angular momentum Clebsch-Gordan coefficients (see Eq. (2) in [36]). There are two important remarks that one has to make here. First, the B_{LS} amplitudes from the fit have already been redefined in order to account for the helicity couplings from the strong decays $\Lambda^* \to K^- p$; i.e., the experiment reports values for the products $H_{\lambda_2,\lambda_{J/\psi}}(\Lambda_b^0 \to \Lambda^* J/\psi) H_{+1/2}(\Lambda^* \to K^- p)$. It is obvious that the additional factor $H_{+1/2}(\Lambda_n^\star \to K^- p)$ still allows one to compare the moduli of normalized helicity amplitudes with theoretical expectations. The second remark concerns the unusual sign of the helicity λ_p in the $\Lambda^\star$ decay chain in [37] leading to a redefinition $H_{\lambda_\Lambda^\star,\lambda_{J/\psi}}(\Lambda_b^0 \to \Lambda_n^\star J/\psi) \to (\pm)(H_{-\lambda_\Lambda^\star,-\lambda_{J/\psi}}(\Lambda_b^0 \to \Lambda_n^\star J/\psi)^*$.

In Tables V and VI, we compare our predictions for the moduli squared of normalized helicity amplitudes with values recalculated from a fit to experimental data [37]. Unfortunately, the absence of the correlation matrix does not allow us to estimate the error bands for those values; nevertheless, they are expected to be rather large. We found that the predicted values of $H_{\lambda_\Lambda^\star,\lambda_{J/\psi}}$ do not vary significantly with the invariant mass $M(Kp)$ and the leading contribution should come from the $H_{-1/2,0}$ and $H_{-1/2,-1}$ helicity amplitudes for both the $J^P = \frac{1}{2}^\pm$ and $\frac{3}{2}^\pm$ cases. No

TABLE V. Asymmetry parameters and moduli squared of normalized helicity amplitudes $|\hat{H}_{\lambda_{\Lambda^\star}\lambda_\psi}|^2$ for the $\Lambda_b^0 \to \Lambda^\star(\frac{1}{2}^\pm)$ transition.

$\Lambda^{(\star)}$, J^P	$\Lambda(1405)$, $\frac{1}{2}^-$		$\Lambda(1600)$, $\frac{1}{2}^+$		$\Lambda(1800)$, $\frac{1}{2}^-$		$\Lambda(1810)$, $\frac{1}{2}^+$	
Quantity	Our results	LHCb [37]	Our results	LHCb [37]	Our results	LHCb [37]	Our results	LHCb [37]
$\lvert\hat{H}_{+\frac{1}{2}+1}\rvert^2$	1.27×10^{-2}	$0.0254.08 \times 10^{-2}$	0.105	2.33×10^{-2}	0.137	6.90×10^{-2}	0.059	
$\lvert\hat{H}_{+\frac{1}{2}0}\rvert^2$	5.19×10^{-3}	0.241	1.05×10^{-2}	0.085	5.23×10^{-3}	0.176	1.99×10^{-2}	0.243
$\lvert\hat{H}_{-\frac{1}{2}0}\rvert^2$	0.514	0.143	0.458	0.455	0.457	0.422	0.418	0.478
$\lvert\hat{H}_{-\frac{1}{2}-1}\rvert^2$	0.468	0.592	0.491	0.345	0.514	0.266	0.493	0.221
α_b	−0.054	0.665	0.003	−0.130	0.039	−0.117	0.026	−0.073
r_0	0.519	0.384	0.468	0.540	0.462	0.598	0.438	0.721
r_1	−0.509	0.098	−0.447	−0.370	−0.452	−0.246	−0.398	−0.235

TABLE VI. Asymmetry parameters and moduli squared of normalized helicity amplitudes $|\hat{H}_{\lambda_{\Lambda^\star}\lambda_\psi}|^2$ for the $\Lambda_b^0 \to \Lambda^\star(\frac{3}{2}^\pm)$ transition.

$\Lambda^\star$, J^P	$\Lambda(1520)$, $\frac{3}{2}^-$		$\Lambda(1690)$, $\frac{3}{2}^-$		$\Lambda(1890)$, $\frac{3}{2}^+$	
Quantity	Our results	LHCb [37]	Our results	LHCb [37]	Our results	LHCb [37]
$\lvert\hat{H}_{+\frac{3}{2}+1}\rvert^2$	8.37×10^{-5}	0.067	2.44×10^{-4}	0.054	3.50×10^{-4}	0.297
$\lvert\hat{H}_{+\frac{1}{2}+1}\rvert^2$	2.26×10^{-2}	0.107	4.67×10^{-2}	0.031	3.19×10^{-2}	0.130
$\lvert\hat{H}_{+\frac{1}{2}0}\rvert^2$	1.82×10^{-3}	0.047	4.98×10^{-3}	0.492	1.61×10^{-3}	0.236
$\lvert\hat{H}_{-\frac{1}{2}0}\rvert^2$	0.536	0.552	0.509	0.257	0.512	0.078
$\lvert\hat{H}_{-\frac{1}{2}-1}\rvert^2$	0.439	0.109	0.437	0.040	0.451	0.207
$\lvert\hat{H}_{-\frac{3}{2}-1}\rvert^2$	1.06×10^{-3}	0.119	1.78×10^{-3}	0.126	3.34×10^{-3}	0.053
α_b	−0.118	−0.555	−0.115	0.172	−0.094	0.479
r_0	0.537	0.599	0.514	0.749	0.514	0.314
r_1	−0.534	−0.505	−0.504	0.235	−0.510	0.158

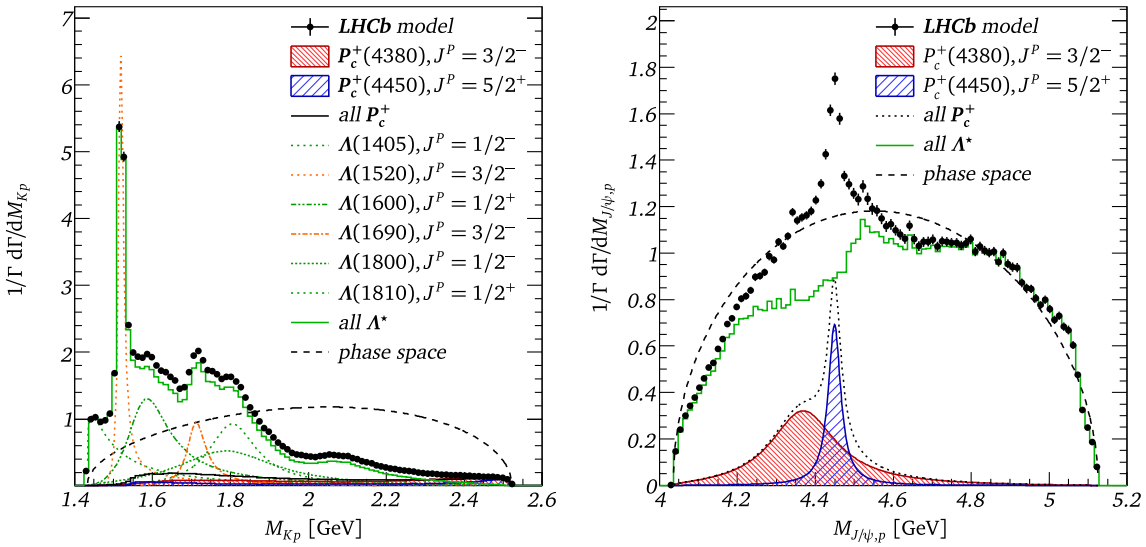

FIG. 1. The invariant mass $M(Kp)$ (left) and $M(J/\psi p)$ (right) distributions. Full LHCb model pseudodata are shown as black dots with error bars, while the hatched area corresponds to the P_c^+ exotic states. The main contributions from the $\Lambda^{(*)}$ resonances are also shown.

such pattern could be found in the experimental data (may be except for r_0).

At this stage we cannot decide definitely whether our theoretical approach contradicts the experimental analysis or not. A refit of the LHCb data using our theoretical restrictions for the helicity amplitudes is needed to obtain an unambiguous conclusion.

Despite this fact, we propose a simple check. For this purpose we have generated a sample of 750k events containing the decay $\Lambda_b^0 \to J/\psi K^- p$ using the PYTHIA 8.1 [40] Monte Carlo generator. The decay products are distributed isotropically in the Λ_b^0 rest frame. We have used an event-by-event reweighting to take into account the presence of resonances as well as possible interference effects between them. The weight is given by the matrix element squared and is calculated for each simulated Λ_b^0 decay using the 4-momenta of the outgoing particles. We have tried to reproduce the default LHCb fit which is known to describe the experimental data well by using the corresponding matrix elements (Eq. (8) from [36]) with the appropriate constants given in [37].

The invariant mass distributions for the $M(Kp)$ and $M(J/\psi p)$ invariant masses are shown in Fig. 1. We have

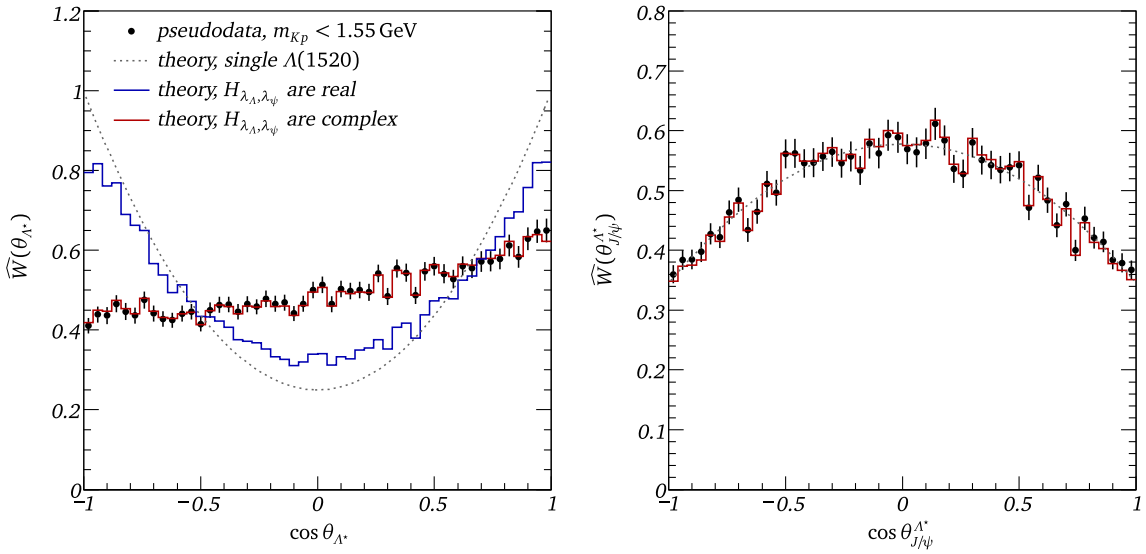

FIG. 2. Helicity angles $\theta_{\Lambda^\star}$ (left) and $\theta_{J/\psi}$ (right) distributions for the low mass M_{Kp} region ($M_{Kp} < 1.55$ GeV). Full LHCb model (pseudodata) is shown as black dots with error bars, while the dotted line represent our calculation for the single $\Lambda(1520)$ state. Solid red and blue lines correspond to our attempt to describe the pseudodata by taking into account only the 3 lowest $\Lambda^\star$ states, see details in text.

concentrated on events with $M(Kp) < 1.55$ GeV where this subsample contains about 39k of the Λ_b^0 decays. The contribution from the $\Lambda(1520)$ state should be dominant here while the influence of P_c^+ pentaquark states can be safely neglected.

Next we have tried to consider the helicity angle distributions for Λ_b^0, $\Lambda^\star$ and J/ψ (our definitions for helicity angles are identical with those of the LHCb analysis). $\hat{W}(\theta_{\Lambda_b^0})$ should be trivial for the decay of a unpolarized Λ_b^0 particle. The shape of the helicity angle $\theta_{J/\psi}$ distribution is the same as for the single resonance: $\hat{W}(\theta_{J/\psi}) = \frac{1}{2}(1 + \frac{A}{2}(3\cos^2\theta_{J/\psi} - 1))$, with a coefficient $A \sim (1 - 3r_0)/2$.

The most interesting distribution $\widehat{W}(\theta_{\Lambda^\star})$ is shown on the left plot in Fig. 2. The black dotted curve corresponds to the full LHCb model. The curve does not look like the expected even function of the cosine of the $\Lambda^\star$ helicity angle. The main reason is the strong interference between different intermediate $\Lambda^\star$ resonances. We have tried to describe this distribution by taking into account only the three lowest $\Lambda^\star$ states (i.e., $\Lambda(1405)$, $\Lambda(1520)$ and $\Lambda(1600)$). We have further neglected all helicity amplitudes except for $H_{-1/2,0}$ and $H_{-1/2,-1}$; the overall fraction of each $\Lambda^\star$ resonance is also fixed to its LHCb values.

In our approach, all helicity amplitudes $H_{\lambda_\Lambda^\star,\lambda_J/\psi}$ are real. Complex phases can result from the decay $\Lambda^\star \to K^- p$ through final state interactions. To start with we assign an identical complex phase to each helicity amplitude. The result is shown on Fig. 2 by a solid blue line. Obviously, it does not agree with the reference plot. One can achieve a reasonable agreement by varying the 5 complex phases of the different helicity amplitudes $H_{\lambda_2\lambda_V}$ and keeping the moduli of the helicity amplitudes $H_{\lambda_2\lambda_V}$ unchanged (see the solid red line in Fig. 2). We take this as evidence that experimental data can in fact be described within our theoretical approach which includes quite strong constraints for the moduli of the helicity amplitudes.

V. SUMMARY

We have calculated the invariant and helicity amplitudes in the transitions $\Lambda_b \to \Lambda^{(*)}(J^P) + J/\psi$, where the $\Lambda^{(*)}(J^P)$ states are (sud)-resonances with J^P quantum numbers $J^P = \frac{1}{2}^\pm, \frac{3}{2}^\pm$. The calculations were performed in the framework of a covariant confined quark model previously developed by us. We have found that the values of the helicity amplitudes for the transitions into the $\Lambda^*(1520, \frac{3}{2}^-)$ and $\Lambda^*(1890, \frac{3}{2}^+)$ states are suppressed compared with those for the transitions into the ground state $\Lambda(1116, \frac{1}{2}^+)$ and the excited state $\Lambda^*(1405, \frac{1}{2}^-)$.

We have compared our numerical results for the helicity amplitudes and decay assymmetry parameters for the set of Λ^* resonances with those recalculated from the LHCb fit. We have shown that the helicity angle distributions for the low-mass Λ^* resonances ($M(Kp) < 1.55$ GeV) can be reproduced using our predicted values for the normalized helicity amplitudes $\hat{H}_{-1/2,0}$ and $\hat{H}_{-1/2,-1}$.

This analysis is important for the identification of the hidden charm pentaquark states $P_c^+(4450)$ and $P_c^+(4380)$ since the cascade decay $\Lambda_b \to \Lambda^*(\frac{1}{2}^-, \frac{3}{2}^\pm)(\to pK^-) + J/\psi$ involves the same final states as the decay $\Lambda_b^0 \to P_c^+(\to pK^-) + J/\psi$.

ACKNOWLEDGMENTS

This work was supported by the German Bundesministerium für Bildung und Forschung (BMBF) under Project No. 05P2015 -ALICE at High Rate (BMBF-FSP 202): Jet- and fragmentation processes at ALICE and the parton structure of nuclei and structure of heavy hadrons, by CONICYT (Chile) PIA/Basal FB0821, by the Tomsk State University Competitiveness Improvement Program and the Russian Federation program "Nauka" (Contract No. 0.1764.GZB.2017). M. A. I. acknowledges the support from the PRISMA cluster of excellence (Mainz Uni.). M. A. I. and J. G. K. thank the Heisenberg-Landau Grant for the partial support. P.S. acknowledges support by the INFN (QFT-HEP project).

[1] R. Aaij *et al.* (LHCb Collaboration), Phys. Lett. B **724**, 27 (2013).
[2] T. Gutsche, M. A. Ivanov, J. G. Körner, V. E. Lyubovitskij, and P. Santorelli, Phys. Rev. D **88**, 114018 (2013).
[3] L. Roca, M. Mai, E. Oset, and U. G. Meiner, Eur. Phys. J. C **75**, 218 (2015).
[4] A. Feijoo, V. K. Magas, A. Ramos, and E. Oset, Phys. Rev. D **92**, 076015 (2015); **95**, 039905(E) (2017).
[5] H. X. Chen, L. S. Geng, W. H. Liang, E. Oset, E. Wang, and J. J. Xie, Phys. Rev. C **93**, 065203 (2016).
[6] E. Wang, H. X. Chen, L. S. Geng, D. M. Li, and E. Oset, Phys. Rev. D **93**, 094001 (2016).
[7] A. Feijoo, V. K. Magas, A. Ramos, and E. Oset, Eur. Phys. J. C **76**, 446 (2016).
[8] J. X. Lu, E. Wang, J. J. Xie, L. S. Geng, and E. Oset, Phys. Rev. D **93**, 094009 (2016).

[9] L. Roca and E. Oset, Eur. Phys. J. C **76**, 591 (2016).
[10] M. Bayar, F. Aceti, F. K. Guo, and E. Oset, Phys. Rev. D **94**, 074039 (2016).
[11] W. Altmannshofer, P. Ball, A. Bharucha, A. J. Buras, D. M. Straub, and M. Wick, J. High Energy Phys. 01 (2009) 019.
[12] A. Faessler, T. Gutsche, M. A. Ivanov, J. G. Körner, and V. E. Lyubovitskij, Phys. Rev. D **80**, 034025 (2009).
[13] R. Lednicky, Yad. Fiz. **43**, 1275 (1986) [Sov. J. Nucl. Phys. **43**, 817 (1986)].
[14] P. Bialas, J. G. Körner, M. Krämer, and K. Zalewski, Z. Phys. C **57**, 115 (1993).
[15] A. Kadeer, J. G. Körner, and U. Moosbrugger, Eur. Phys. J. C **59**, 27 (2009).
[16] M. Nielsen, F. S. Navarra, and S. H. Lee, Phys. Rep. **497**, 41 (2010).
[17] S. Weinberg, Phys. Rev. **130**, 776 (1963).
[18] A. Salam, Nuovo Cimento **25**, 224 (1962).
[19] K. Hayashi, M. Hirayama, T. Muta, N. Seto, and T. Shirafuji, Fortschr. Phys. **15**, 625 (1967).
[20] G. V. Efimov and M. A. Ivanov, *The Quark Confinement Model of Hadrons* (IOP Publishing, Bristol, 1993).
[21] J. A. M. Vermaseren, Nucl. Phys. B, Proc. Suppl. **183**, 19 (2008); arXiv:math-ph/0010025.
[22] M. A. Ivanov, J. G. Körner, and C. T. Tran, Phys. Rev. D **95**, 036021 (2017).
[23] M. A. Ivanov, J. G. Körner, and C. T. Tran, Phys. Rev. D **94**, 094028 (2016).
[24] M. A. Ivanov and C. T. Tran, Phys. Rev. D **92**, 074030 (2015).
[25] M. A. Ivanov, J. G. Körner, and C. T. Tran, Phys. Rev. D **92**, 114022 (2015).
[26] A. Issadykov, M. A. Ivanov, and S. K. Sakhiyev, Phys. Rev. D **91**, 074007 (2015).
[27] S. Dubnička, A. Z. Dubničkov, N. Habyl, M. A. Ivanov, A. Liptaj, and G. S. Nurbakova, Few-Body Syst. **57**, 121 (2016).
[28] S. Dubnička, A. Z. Dubničkov, A. Issadykov, M. A. Ivanov, A. Liptaj, and S. K. Sakhiyev, Phys. Rev. D **93**, 094022 (2016).
[29] T. Gutsche, M. A. Ivanov, J. G. Körner, V. E. Lyubovitskij, P. Santorelli, and N. Habyl, Phys. Rev. D **91**, 074001 (2015); **91**, 119907(E) (2015).
[30] T. Gutsche, M. A. Ivanov, J. G. Körner, V. E. Lyubovitskij, and P. Santorelli, Phys. Rev. D **93**, 034008 (2016).
[31] T. Gutsche, M. A. Ivanov, J. G. Körner, S. Kovalenko, and V. E. Lyubovitskij, Phys. Rev. D **94**, 114030 (2016).
[32] G. Aad *et al.* (ATLAS Collaboration), Phys. Rev. D **89**, 092009 (2014).
[33] CMS Collaboration, Report No. CMS-PAS-BPH-15-002.
[34] V. V. Abramov, Yad. Fiz. **68**, 414 (2005) [Phys. At. Nucl. **68**, 385 (2005)].
[35] G. Hiller, M. Knecht, F. Legger, and T. Schietinger, Phys. Lett. B **649**, 152 (2007).
[36] R. Aaij *et al.* (LHCb Collaboration), Phys. Rev. Lett. **115**, 072001 (2015).
[37] N. P. Jurik, Report No. CERN-THESIS-2016-086.
[38] A. D. Martin and T. D. Spearman, *Elementary Particle Theory* (North-Holland, Amsterdam, 1970).
[39] S. U. Chung, CERN Yellow Report No. 71-8, 1971.
[40] T. Sjostrand, S. Mrenna, and P. Z. Skands, Comput. Phys. Commun. **178**, 852 (2008).